

Photoinduced C-C Coupling | Very Important Paper |

VIP

# Investigation of Straightforward, Photoinduced Alkylations of Electron-Rich Heterocompounds with Electron-Deficient Alkyl Bromides in the Sole Presence of 2,6-Lutidine

Elina Fuks,<sup>[a]</sup> Laura Huber,<sup>[a]</sup> Thea Schinkel,<sup>[a]</sup> and Oliver Trapp<sup>\*,[a,b]</sup>

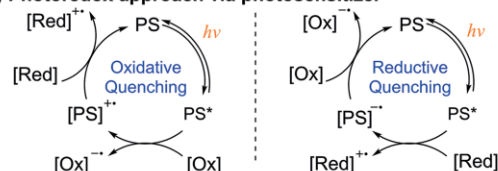
**Abstract:** Alkylations of simple electron-rich heterocompounds deliver valuable target structures in bioorganic and medicinal chemistry. Herein, we present a straightforward and photosensitizer free approach for the photoinduced C–C coupling of electron-rich unsaturated heterocompounds with alkyl bromides using 405 nm and 365 nm irradiation. Comprehensive mechanistic studies indicate the involvement of 2,6-lutidine in the formation of a non-covalently bound intermediate to which the function of a photosensitizer is attributed. UV/Vis spectra reveal the formation of a bathochromic shifted band when the elec-

tron-deficient alkyl bromide is mixed with the structural motif of 2,6-substituted pyridine. Upon photochemical excitation of this band, we find the initiation of the C–C bond-forming reaction. Using this approach highly versatile alkylation products, e.g.  $\alpha$ -substituted ketones and 2-substituted furan, thiophene, and pyrrole derivatives, are obtained in high selectivity. Furthermore, this synthetic methodology can be applied to access substituted indoles, which cannot be obtained by other transformations.

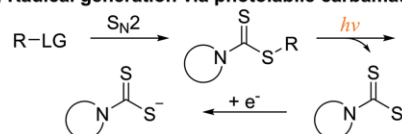
Selective and direct chemical transformations under benign reaction conditions using sustainable energy resources are highly sought-after. The easy handling and continuous availability of light along with the creation of novel reaction pathways have been stimulating the interest in photochemical transformations for a century.<sup>[1]</sup> MacMillan,<sup>[2,3]</sup> Yoon<sup>[4]</sup> and Stephenson<sup>[5]</sup> developed and successfully applied visible light-assisted photoredox catalysis to tackle different synthetic challenges. To overcome low absorption efficiencies in these light-mediated transformations, photosensitizers (PS) for light energy transfer were implemented (Scheme 1; I).<sup>[6]</sup> Based on this activation strategy, numerous reports on light-triggered processes involving ruthenium<sup>[7]</sup> and iridium pyridyl complexes<sup>[8]</sup> as well as metal-free dyes<sup>[9]</sup> have been published to date. Such chromophores exhibit high extinction coefficients, are photostable and efficient in energy transfer, and therefore enable a broad range of applications. However, the design of new chromophore-assisted photocatalytic cycles is time-consuming due to the re-

## Strategies to light-assisted alkylations

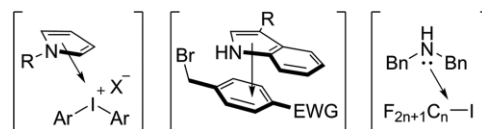
### I) Photoredox approach via photosensitizer



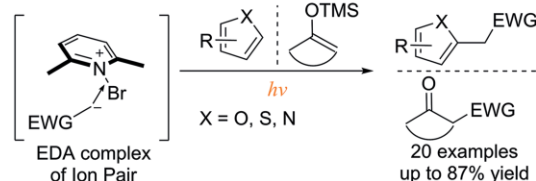
### II) Radical generation via photolabile carbamates



### III) Selected examples of identified EDA complexes



### IV) This work: Involvement of 2,6-lutidine in EDA complexes



[a] E. Fuks, L. Huber, T. Schinkel, Prof. Dr. O. Trapp  
Department of Chemistry, Ludwig Maximilian University Munich  
Butenandstr. 5-13, 81377 Munich, Germany  
E-mail: oliver.trapp@cup.uni-muenchen.de  
<https://www.cup.lmu.de/oc/trapp/>

[b] Prof. Dr. O. Trapp  
Max-Planck-Institute for Astronomy  
Königstuhl 17, 69117 Heidelberg, Germany

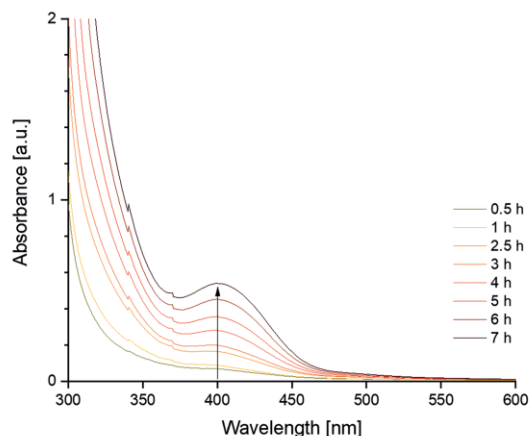
Supporting information and ORCID(s) from the author(s) for this article are available on the WWW under <https://doi.org/10.1002/ejoc.202001003>.

© 2020 The Authors published by Wiley-VCH GmbH. This is an open access article under the terms of the Creative Commons Attribution-NonCommercial License, which permits use, distribution and reproduction in any medium, provided the original work is properly cited and is not used for commercial purposes.

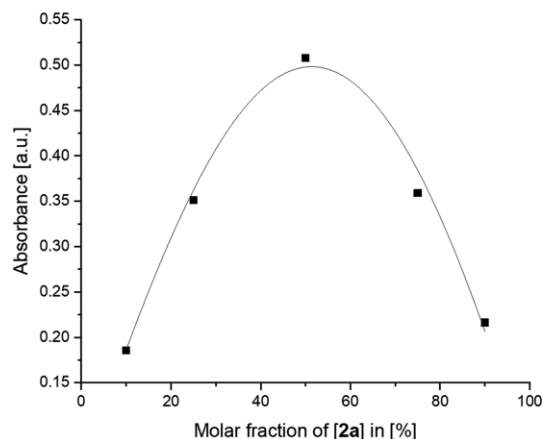
Scheme 1. Overview of possible activation modes for light-assisted alkylations. I) Dual photoredox catalysis using a photosensitizer. II) Generation of radicals via a photolabile dithiocarbamate. III) Recent examples for EDA complexes including donor substrates (left, central) and external sacrificial donor (right). IV) Alkylations of electron-deficient alkyl bromides with electron-rich heterocompounds in the presence of 2,6-lutidine presented in this work.



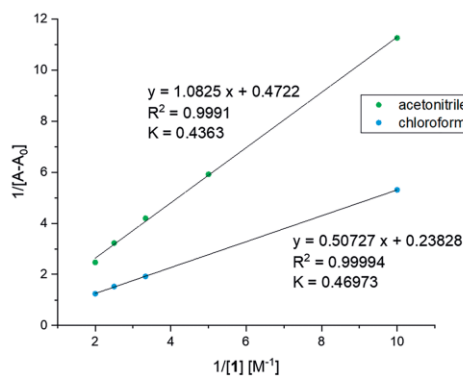
**a) UV-Vis of 1:1 mixture of 2,6-lutidine and bromoacetonitrile**



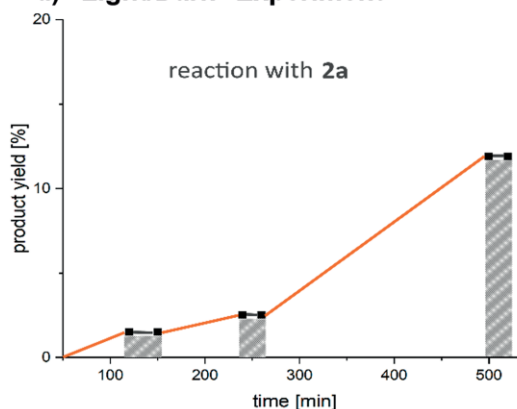
**b) Job Plot**



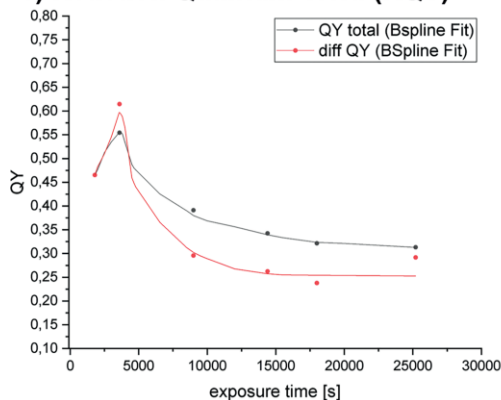
**c) Benesi-Hildebrand Measurement**



**d) "Light/Dark" Experiment**



**e) Reaction Quantum Yield (RQY)**



**f) Comparative UV-Vis Experiments**

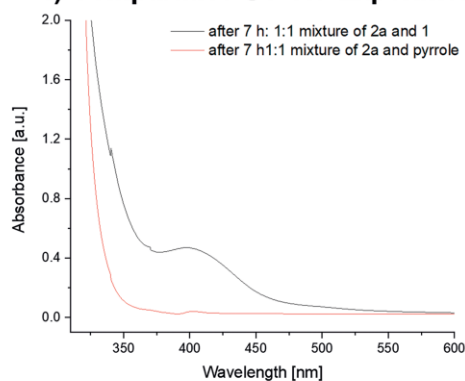


Figure 1. Mechanistic studies. a) Time resolved UV/Vis measurement of 1:1 mixture of 2,6-lutidine (**1**) and bromoacetonitrile (**2a**) with  $\lambda_{\text{max}} = 400 \text{ nm}$ . b) Job plot of **2a** and **1**. The maximum of the measured Job plot is at 50 % molar fraction of **2a**. c) Linearized Benesi-Hildebrand plot of **1** and **2a** in acetonitrile and chloroform. d) Product yield dependency of alternating dark/light cycles in the reaction of **2a**. Grey rectangles illustrate dark periods and the orange lines represent irradiation periods. e) Plots of the total quantum yield (QY) in black, calculated after the given time, and the differential quantum yield (diffQY) in red, related to the time intervals between the measurements, against irradiation time in seconds. Both graphs refer to the reaction of **2a**. f) Graphic comparison of UV/Vis experiments with **2a** after 7 hours: 1:1 mixture of **2a** and **1** (black) and 1:1 mixture of **2a** and pyrrole (red).

employing the spectroscopic Benesi-Hildebrand method, we were able to quantify the corresponding association constants  $K = 0.47 \text{ M}^{-1}$  in chloroform and  $K = 0.44 \text{ M}^{-1}$  in acetonitrile (Fig-

ure 1c). These results are in excellent agreement with literature data for an inner sphere electron transfer, which is typically characterized by a stronger stabilization compared to an outer

sphere event.<sup>[22]</sup> To exclude experimental artifacts from the involvement of a colored covalently bound intermediate, we synthesized the crystalline *N*-cyanomethyl-2,6-lutidinium bromide salt and measured its absorption spectra (Supporting Information, Figure S3, and XRD structure Figure S21). We did not detect any band in the visible range, which implies that the reaction does not proceed via the nucleophilic substitution of the bromide. Additional confirmation was obtained when the alkyl bromide was replaced by the *N*-cyanomethyl-2,6-lutidinium bromide salt and no alkylated product was formed.

We further conducted several <sup>1</sup>H-NMR measurements of the reaction mixtures and of the colored two-component solutions of **1** and **2a**. We observed defined spectra with no evidence for any side products which might emerge from termination of radicals or from an organic chemical reaction not considered (Supporting Information Figures S13 and S14). Our findings establish the presence of an associative interaction, namely an EDA complex.

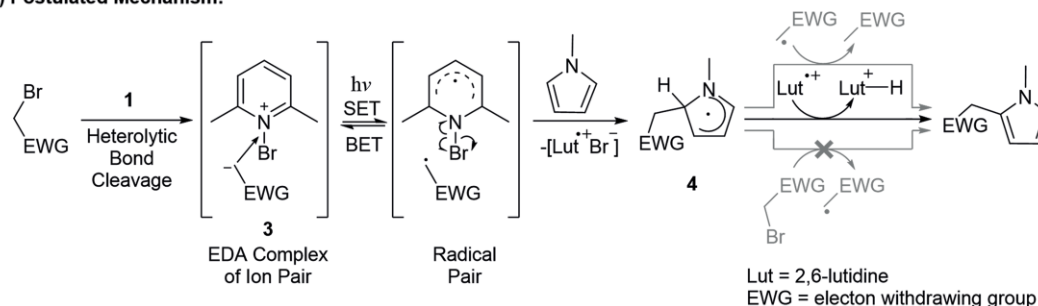
We studied the steric effect of 2,6-substituted pyridines on product formation, as steric hindrance restricts an approximation between the nucleophile (or donor) and electrophile (or acceptor). Reduced yields of the  $\alpha$ -alkylated product were obtained in the sequence of isobutyl, *tert*-butyl and isopropyl residues, which further confirms the direct participation of pyridine derivatives in the activation process. Better nucleophiles such as 2-methylpyridine and pyridine afforded the non-reactive pyridinium salt by substitution of the bromide in **2a**. To further investigate the role of light, we performed alternating light and

dark cycles (Figure 1d). During the dark periods, no change in yield was observed, while upon irradiation, the product formation continued and afforded similar yields compared to constant irradiation in the same time interval. The experiment emphasizes the necessity of light for reaction conversion and at the same time excludes a radical chain mechanism of long chains.

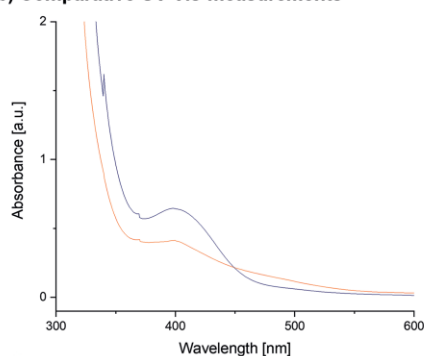
A more profound mechanistic understanding was obtained by the determination of the quantum yield under oxygen-free conditions using the spectroscopic apparatus developed by König and Riedle.<sup>[23]</sup> When selecting the experimental setup, we were guided by the literature.<sup>[24,25]</sup> We observed a time-dependency of the quantum yield with a maximum of  $\Phi = 0.56$  after 1 hour of irradiation, followed by an exponential decrease and stabilization at  $\Phi = 0.31$  for long term exposure of 5–13 h (Figure 1e). The initial increase is presumably the result of an induction phase, in which the EDA complex is formed. At no time was the limit of  $\Phi = 1$  exceeded, which indicates either a low efficiency of the initiation of a radical-chain reaction or the complete absence of a radical-chain reaction.<sup>[26,27]</sup>

With regard to the slow visible band formation and the high oxidation potential of pyridine-based structures [ $E_{\text{ox}}(\text{Pyr}^+/\text{Pyr}) = 2.2 \text{ V vs. SCE}$ ],<sup>[28]</sup> we excluded a direct EDA complex from **1** and **2a**. In contrast, the EDA complex **3** of the redox-active *N*-bromolutidinium cation and the alkyl anion is in agreement with the presented results and electrochemical considerations. The generation of **3** is initiated by the nucleophilic attack of **1** on the bromine atom with concomitant heterolytic cleavage of

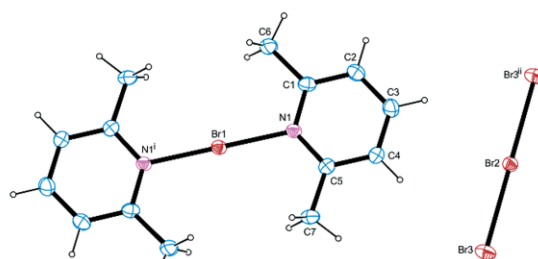
#### a) Postulated Mechanism:



#### b) Comparative UV-Vis measurements



#### c) Crystal Structure of **5**



Scheme 3. a) Proposed mechanism of the photoreaction of 2,6-lutidine (**1**) with the electron-deficient alkyl bromide (**2**). The heterolytic cleavage of the C–Br bond of **2** by the nucleophilic attack of **1** results in the formation of the EDA complex **3**. Upon irradiation a single electron transfer (SET) is induced leading to a radical pair. Concomitant with the fragmentation of the *N*-bromolutidyl radical, the carbon-centered radical is intercepted by the nucleophile to produce **4**. Oxidative rearomatization by the lutidinium radical cation affords the alkylated product. Less operative reaction pathways are shown in grey. b) Comparative UV/Vis spectra of 0.84 mM solution of **5** (orange) and an equimolar mixture of solution of **1** and **2a** after 5 h (blue) c) Crystal structure of **5**.

**2a**. Upon the photochemical excitation of the complex **3** an electron transfer is triggered resulting in a radical pair comprised of the *N*-bromolutidyl radical and the resonance-stabilized alkyl radical. In the next step, the reduced lutidyl scaffold undergoes a N–Br bond fragmentation to liberate the lutidinium radical cation and bromide anion. Subsequently, the carbon centered radical is intercepted by the nucleophile forming the radical species **4**. The reaction sequence is completed by oxidative rearomatization, which most likely involves the previously generated 2,6-lutidinium radical cation, as there is no evidence for debromination, or termination products associated with a radical-chain reaction. This assumption is also consistent with the observation, that for higher concentrated reaction solutions we were able to isolate and identify the precipitated lutidinium bromide. The postulated mechanism is illustrated in Scheme 3a.

We have demonstrated the feasibility of the nucleophilic attack of 2,6-lutidine towards the bromine atom within the bromonium-2,6-lutidine association by isolating the crystal structure of the intensively colored, bis-coordinate complex **5** from **1** and elemental bromine (Scheme 3c). This light-sensitive complex has been described previously in the literature as a photoinitiator or mild brominating reagent.<sup>[29]</sup> Interestingly, we observed an almost identical absorption band with  $\lambda_{\text{max}} = 400$  nm compared to the one obtained from the equimolar mixture of **1** and **2a** (Scheme 3b). However, the involvement of this bis-coordinate complex in the reaction process can be excluded for several reasons. Firstly, in solutions of alkyl bromides **2** in chloroform no coloration was visible even after 24 hours (Supporting Information, Figure S4), which indicates the absence of the elemental bromine as an impurity or decomposition product. Secondly, when catalytic amounts of the complex **5** (0.2 equiv.) were added to the reaction, a mixture of the product (12 %) and the 2-bromopyrrole was observed. Under standard reaction conditions, no brominated compounds were detected. Additionally, absorption spectra of 2,6-lutidine mixtures with **2a** and **2b** differ in the position of the absorption maxima, thus indicating the formation of two unequal EDA complexes.

The reactivity of *N*-substituted pyridinium salts for reductive fragmentation, as postulated in the mechanism, was studied in detail elsewhere and was outlined recently in a review.<sup>[30]</sup>

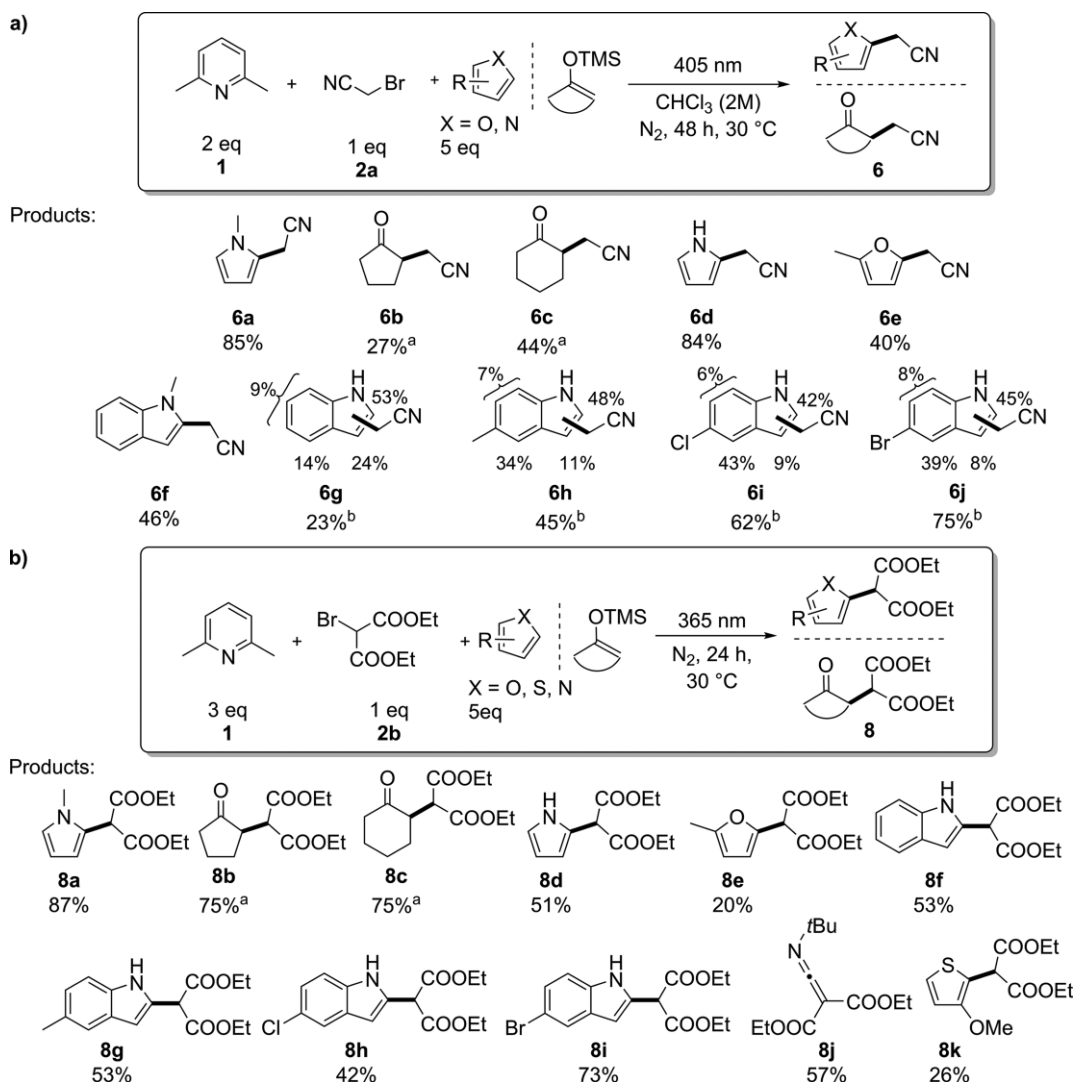
Next, we conducted a series of optimization and control experiments to prove the necessity of individual reaction components. As already pointed out, in the dark no product formation was observed. The conversion was strongly dependent on the intensity of the LED lamp and the high concentration of 2 M of **2a** in the reaction with *N*-methylpyrrole. Noteworthy, we have experimentally verified the correlation between the power [W] and the light intensity [counts] for the LED lamps used (Supporting Information, Figure S1). After 24 h of light exposure, a high yield of 88 % was obtained under inert conditions. However, higher yields were detected after 48 h of irradiation. The use of fewer equivalents of *N*-methylpyrrole (2–4 equiv.) resulted in lower yields down to 70 % after 24 h, whereas no reaction was observed for 1 equivalent (Supporting Information, p. 18). These results illustrate the necessity of at least a

fivefold excess of the nucleophile for a sufficient reaction rate when intercepting the electron-poor radical. Heating the solution to 30 °C, caused by permanent irradiation over 24 h, was essential for conversion. In the presence of oxygen, a similar yield was achieved in a highly selective reaction after an induction phase of several hours. However, we consistently observed the precipitation of a dark solid under air atmosphere, which is most likely due to the oxidation of pyrrole to polypyrrole. Their potential as in situ formed photosensitizers, which has only recently been demonstrated, might explain the successful conversion under aerobic conditions.<sup>[31]</sup>

To further support the mechanism of the proposed EDA complex activation and in an effort to broaden the synthetic applicability, we studied a variety of compounds as potential radical traps. Therefore, we extended our optimized reaction conditions to further unsaturated nucleophiles (Scheme 4a) according to the Mayr scale.<sup>[21]</sup> Trimethylsilyl ethers were also compatible with the coupling conditions and provided  $\alpha$ -substituted ketones **6b** and **6c** in yields of up to 44 %. Unprotected pyrrole gave the coupled product **6d** in a good yield of 84 %. Successful conversion was further achieved with electron-rich heteroaromatics such as 2-methylfuran (40 % yield of **6e**), and indole derivatives with overall yields between 12 % and 46 % (**6f–j**) for a mixture of constitutional isomers. The evaluation of the regioselectivity for indole derivatives showed a preferential addition to the 2- and 4-ring positions in almost equal distribution of 40–48 %, respectively. We succeeded in obtaining a crystal structure of one of the two purified principle products of **7**, which confirms the structural assignment for the substitution in 4-position. In contrast, only the 2-position with 53 % was favored for indole. The isomer distribution of the products demonstrates that the mechanism deviates from the conventional  $S_E$  attack of the 3-position and confirms the involvement of radicals.<sup>[32]</sup> Notably, indole halides were tolerated in the photo-reaction and the unreacted substrate could be recovered. Highly reactive diazo compounds and substrates without a vicinal double bond with respect to the heteroatom such as *tert*-butyl isocyanide were incompatible in this reaction. The reactivity limit for **2a** was reached with 3-methoxythiophene at a nucleophilicity value of  $N = 3.06$ .<sup>[33]</sup> The product scope is in agreement with the proposed mechanism, as product formation is interlinked with the electronic nature of radical traps.

Similar spectroscopic results were obtained with the second bromine-bearing radical precursor, diethyl bromomalonate (**2b**), which is commonly used in photochemical transformations. When **2b** was added to 2,6-lutidine, a new absorption band with  $\lambda_{\text{max}} = 416$  nm appeared (Supporting Information, Figure S7). The characteristics of the absorption band were analogous to the substrate **2a**, providing strong evidence for the involvement of a further EDA complex, i.e. an association of the electronically counter-polarized molecules. We determined an association constant of  $K = 0.35 \text{ M}^{-1}$  in chloroform (Supporting Information, Figure S12). Due to the low conversion rates in the spectroscopic setup of König and Riedle,<sup>[23]</sup> a long-term measurement of the quantum yield turned out to be error-prone. We monitored the formation of colored, unidentifiable photo-degradation products during long exposure times.





Scheme 4. Reaction Scope of the optimized photoreactions. Depicted yields indicate isolated and purified products. The newly formed C–C bond is illustrated in bold. a) Photoreaction of bromoacetonitrile. b) Photoreaction of bromomalonate. [a] Racemic product. [b] Regio isomer probability is indicated in percent next to the position and the overall isolated yield is given below.

We then successfully incorporated the association of **2b** and **1** into the photo-functionalization. For the reactions with **2b** high optical intensities and substrate concentrations were necessary. For the coupling to liquid nucleophiles, the absence of a solvent was decisive. In the case of indole as a solid substrate, chloroform was added until complete dissolution. The highest conversion was achieved with a highly intense 11 W 365 nm LED lamp, while the 3 W 405 nm LED was not productive. One explanation for the lack of conversion during irradiation of the visible band could be an efficient back electron transfer (BET) leading to the regeneration of the EDA ground state. In contrast, the irradiation wavelength of 365 nm is in the region of the absorption band tail of the EDA complex comprised of pyrrole (Prr) and **2b** (Supporting Information, Figure S5). We assume that photochemical excitation of this EDA complex induces a SET from the electron-rich donor [ $E_{ox}(Prr^{+}/Prr) = 1.20$  V vs. SCE in MeCN]<sup>[34]</sup> to the alkyl bromide acceptor [ $E_{red}(2b/2b^{-}) = -0.62$  V vs. SCE in MeCN]<sup>[35]</sup> with concomitant fragmentation of

the C–Br bond. The suggested alternative activation pathway involving electron-rich nucleophiles represents a plausible scenario for the generation of malonyl radicals under 365 nm irradiation (Scheme 4b). High yields were obtained for *N*-methyl pyrrole (87 % of **8a**) and both investigated cyclic trimethylsilyl ethers (75 % of **8b**, 75 % of **8c**). For pyrrole and 2-methylfuran, diminished yields of **8d** (51 %) and **8e** (20 %) compared to the cyano-methylated products **6d** (84 %) and **6e** (40 %) were observed. Furthermore, we were able to alkylate *tert*-butyl isocyanide in 57 % yield, forming vinyl imine **8j**. Indole and the 5-substituted indole derivative showed regioselectivity for the 2-position due to steric hindrance of the bulky malonyl residue, resulting in yields of 42–73 % (**8f–h**) obtained as single isomers. In the case of the least nucleophilic substrate, the 3-methoxythiophene, a yield of 26 % (**8k**) was achieved. The difference in product range between the two radical precursors demonstrates the importance of the electronic match of the reactants in this photoinitiated transformation. For highly electron-deficient substrate radi-

cals, less reactive nucleophiles are accessible. In the case of the nucleophilic diazo substrates, a nitrogen loss and the formation of diethyl malonate by debromination was observed.

In summary, we demonstrated a straightforward approach to C–C cross-coupling of electron-rich unsaturated heterocompounds with electron-deficient alkyl bromides under 405 nm or 365 nm irradiation in the presence of 2,6-lutidine. Notably, the here presented methodology does not require an additional photosensitizer. Another advantage is the simple removal of 2,6-lutidine from the reaction mixture, which facilitates the product purification. We have presented detailed mechanistic studies and spectroscopic evidence, which strongly suggest the formation of an EDA complex from the in situ formed *N*-bromo-2,6-alkylated pyridine cations and the anion of electron-poor alkyl bromides. Irradiation near the absorption maximum of the bathochromically shifted band triggered the photoreaction, which resulted in synthetically valuable C–H functionalizations. Alkylated products were isolated in good to high yields for substrates such as trimethylsilyl ethers and derivatives of pyrrole, furan, thiophene, and indole, and further expansion of the methodology to more complex products are underway.

#### Conflict of Interest

The authors declare no conflict of interest.

#### Acknowledgments

We acknowledge financial support from the Ludwig-Maximilians-University Munich, the Max-Planck-Society (Max-Planck-Fellow Research Group Origins of Life), the Deutsche Forschungsgemeinschaft DFG (INST 86/1807-1 FUGG) and the Volkswagen Stiftung (Initiating molecular Life). We thank Dr. Peter Mayer for the X-ray structure analysis. Open access funding enabled and organized by Projekt DEAL.

**Keywords:** Alkylation · C–H functionalization · Photochemistry · Radicals · Synthetic methods

- [1] a) G. Ciamician, *Science* **1912**, 36, 385–394; for reviews on photochemistry see: b) J. M. R. Narayanam, C. R. J. Stephenson, *Chem. Soc. Rev.* **2011**, 40, 102–113; c) N. Hoffmann, *Chem. Rev.* **2008**, 108, 1052–1103; d) M. Fagnoni, D. Dondi, D. Ravelli, A. Albini, *Chem. Rev.* **2007**, 107, 2725–2756.
- [2] T. D. Beeson, A. Mastracchio, J.-B. Hong, K. Ashton, D. W. C. MacMillan, *Science* **2007**, 316, 582–585.
- [3] D. W. C. MacMillan, *Nature* **2008**, 455, 304–308.
- [4] M. A. Ischay, M. E. Anzovino, J. Du, T. P. Yoon, *J. Am. Chem. Soc.* **2008**, 130, 12886–12887.
- [5] J. M. R. Narayanam, J. W. Tucker, C. R. J. Stephenson, *J. Am. Chem. Soc.* **2009**, 131, 8756–8757.
- [6] N. A. Romero, D. A. Nicewicz, *Chem. Rev.* **2016**, 116, 10075–10166.
- [7] a) C. K. Prier, D. A. Rankic, D. W. C. MacMillan, *Chem. Rev.* **2013**, 113, 5322–5363; b) F. Teplý, *Collect. Czech. Chem. Commun.* **2011**, 76, 859–917.
- [8] a) A. G. Condie, J. C. González-Gómez, C. R. J. Stephenson, *J. Am. Chem. Soc.* **2010**, 132, 1464–1465; b) D. Staveness, I. Bosque, C. R. J. Stephenson, *Acc. Chem. Res.* **2016**, 49, 2295–2306; c) C. J. O'Brien, D. G. Droege, A. Y. Jui, S. S. Gandhi, N. A. Paras, S. H. Olson, J. Conrad, *J. Org. Chem.* **2018**, 83, 8926–8935.
- [9] a) M. Neumann, S. Földner, B. König, K. Zeitler, *Angew. Chem. Int. Ed.* **2011**, 50, 951–954; *Angew. Chem.* **2011**, 123, 981–985; b) K. Zeitler, *Angew. Chem. Int. Ed.* **2009**, 48, 9785–9789; *Angew. Chem.* **2009**, 121, 9969–9974; c) I. Ghosh, T. Ghosh, J. I. Bardagi, B. König, *Science* **2014**, 346, 725–728; d) C. Bottecchia, R. Martín, I. Abdaji, E. Crovini, J. Alcazar, J. Orduna, M. J. Blesa, J. R. Carrillo, P. Prieto, T. Noël, *Adv. Synth. Catal.* **2019**, 361, 945–950.
- [10] B. Schweitzer-Chaput, M. A. Horwitz, E. de Pedro Beato, P. Melchiorre, *Nat. Chem.* **2019**, 11, 129–135.
- [11] D. Spinnato, B. Schweitzer-Chaput, G. Goti, M. Ošeka, P. Melchiorre, *Angew. Chem. Int. Ed.* **2020**, 59, 9485–9490; *Angew. Chem.* **2020**, 132, 9572–9577.
- [12] M. Tobisu, T. Furukawa, N. Chatani, *Chem. Lett.* **2013**, 42, 1203–1205.
- [13] S. R. Kandukuri, A. Bahamonde, I. Chatterjee, I. D. Jurberg, E. C. Escudero-Adán, P. Melchiorre, *Angew. Chem. Int. Ed.* **2015**, 54, 1485–1489; *Angew. Chem.* **2015**, 127, 1505–1509.
- [14] X. Sun, W. Wang, Y. Li, J. Ma, S. Yu, *Org. Lett.* **2016**, 18, 4638–4641.
- [15] Further selected examples: a) E. Arceo, I. D. Jurberg, A. Álvarez-Fernández, P. Melchiorre, *Nat. Chem.* **2013**, 5, 750; b) M. Nappi, G. Bergonzini, P. Melchiorre, *Angew. Chem. Int. Ed.* **2014**, 53, 4921–4925; *Angew. Chem.* **2014**, 126, 5021; c) Ł. Woźniak, J. J. Murphy, P. Melchiorre, *J. Am. Chem. Soc.* **2015**, 137, 5678–5681; d) H.-H. Zhang, S. Yu, *Org. Lett.* **2019**, 21, 3711–3715; e) S. Xie, D. Li, H. Huang, F. Zhang, Y. Chen, *J. Am. Chem. Soc.* **2019**, 141, 16237–16242.
- [16] J. Wu, P. S. Grant, X. Li, A. Noble, V. K. Aggarwal, *Angew. Chem. Int. Ed.* **2019**, 58, 5697–5701; *Angew. Chem.* **2019**, 131, 5753.
- [17] a) F. Sandfort, F. Strieth-Kalthoff, F. J. R. Klauck, M. J. James, F. Glorius, *Chem. Eur. J.* **2018**, 24, 17210–17214; b) M. J. James, F. Strieth-Kalthoff, F. Sandfort, F. J. R. Klauck, F. Wagener, F. Glorius, *Chem. Eur. J.* **2019**, 25, 8240–8244.
- [18] M.-C. Fu, R. Shang, B. Zhao, B. Wang, Y. Fu, *Science* **2019**, 363, 1429–1434.
- [19] G. E. M. Crisenza, D. Mazzarella, P. Melchiorre, *J. Am. Chem. Soc.* **2020**, 142, 5461–5476.
- [20] A. C. Closs, E. Fuks, M. Bechtel, O. Trapp, *Chem. Eur. J.* <https://doi.org/10.1002/chem.202001514>.
- [21] a) S. Lakhdar, B. Maji, H. Mayr, *Angew. Chem. Int. Ed.* **2012**, 51, 5739–5742; *Angew. Chem.* **2012**, 124, 5837; b) H. Mayr, T. Bug, M. F. Gotta, N. Hering, B. Irrgang, B. Janker, B. Kempf, R. Loos, A. R. Ofial, G. Remennikov, H. Schimmel, *J. Am. Chem. Soc.* **2001**, 123, 9500–9512.
- [22] C. G. S. Lima, T. de M. Lima, M. Duarte, I. D. Jurberg, M. W. Paixão, *ACS Catal.* **2016**, 6, 1389–1407.
- [23] U. Megerle, R. Lechner, B. König, E. Riedle, *Photochem. Photobiol. Sci.* **2010**, 9, 1400–1406.
- [24] A. Gervien, P. Mayer, H. Dube, *Nat. Commun.* **2019**, 10, 4449.
- [25] J. Tucher, S. Schlicht, F. Kollhoff, C. Streib, *Dalton Trans.* **2014**, 43, 17029–17033.
- [26] L. Buzzetti, G. E. M. Crisenza, P. Melchiorre, *Angew. Chem. Int. Ed.* **2019**, 58, 3730–3747; *Angew. Chem.* **2019**, 131, 3768.
- [27] M. Cismesia, T. P. Yoon, *Chem. Sci.* **2015**, 6, 5426–5434.
- [28] S. R. Waldvogel in *Fundamentals and Applications of Organic Electrochemistry. Synthesis, Materials, Devices*. (Eds.: T. Fuchigami, M. Atobe, S. Inagi), Wiley & Sons, Ltd. **2015**.
- [29] a) M. K. Mishra, S. Lenka, P. L. Nayak, *J. Polym. Sci. Pol. Chem.* **1981**, 19, 2457–2464; b) W. K.-D. Brill, C. Riva-Toniolo, *Tetrahedron Lett.* **2001**, 42, 6279–6282.
- [30] S. L. Rössler, B. J. Jelier, E. Magnier, G. Dagousset, E. M. Carreira, A. Togni, *Angew. Chem. Int. Ed.* **2020**, 59, 9264–9280; *Angew. Chem.* **2020**, 132, 9350–9366.
- [31] Z.-J. Li, S. Li, E. Hofman, A. H. Davis, G. Leem, W. Zheng, *Green Chem.* **2020**, 22, 1911–1918.
- [32] R. J. Sundberg in *Heterocyclic Scaffolds II: Reactions and Applications of Indoles*, Vol. 26 (Ed.: B. U. W. Maes), Springer-Verlag Berlin Heidelberg, **2011**, p. 47–115.
- [33] G. Berionni, V. Morozova, M. Heininger, P. Mayer, P. Knochel, H. Mayr, *J. Am. Chem. Soc.* **2013**, 135, 6317–6324.
- [34] Converted to SCE from A. F. Diaz, A. Martinez, K. K. Kanazawa, *J. Electroanal. Chem.* **1981**, 130, 181–187.
- [35] H. G. Roth, N. A. Romero, D. A. Nicewicz, *Synlett* **2016**, 27, 714–723.

Received: July 21, 2020